

# Design of Sensorless Controlled IPMSM with Concentrated Winding for EV Drive at Low speed

Myung-Seop Lim<sup>1</sup>, Seung-Hee Chai<sup>1</sup> and Jung-Pyo Hong<sup>1</sup>, *Senior Member, IEEE*  
<sup>1</sup>*Department of Automotive Engineering, Hanyang University, Seoul 133-791, Korea*

---

## Abstract

The sensorless control based on the high frequency voltage signal injection method is typically used for detecting the rotor position of an interior permanent magnet synchronous motor (IPMSM). This technique is essential at zero and low speed operating region, where back electromotive force is extremely low. The sensorless-oriented machines require the same minimum value positions of the  $d$ -axis self-inductances, regardless of the rotor position. It means that the zero-crossing points of the  $dq$ -axis mutual-inductances varied with the rotor position should be constant as well. This paper introduces the design procedure of a saliency-based sensorless controlled concentrated winding IPMSM for vehicle traction, fulfilling the requirements mentioned above. The evaluating process of the sensorless drive feasibility by using finite element analysis (FEA) is proposed, with taking account of cross-coupling effect and saturation. Utilizing the evaluating method, some geometry design parameters are examined to figure out which ones have a positive effect on detecting the rotor position. Based on the influences of the parameters on the drive feasibility, the design conditions for the sensorless drive concentrated winding IPMSM are determined. Finally, the proposed model applied with the geometry design conditions and the FEA results are shown. It is found that accuracy of the rotor position estimation is improved by means of the proper geometry design of the machines.

*Keywords: cross-coupling effect, high frequency voltage signal injection, sensorless drive, spatial saliency*

---

## 1 Introduction

An interior permanent magnet synchronous motor (IPMSM) is generally employed as electric vehicle (EV) drive application because of its high power and torque density. For vector control of the machines, the position sensors are essential. However, it increases the motor cost and volume, and decrease reliability of the systems. In addition, using the position sensor could be a latent critical defect of an IPMSM in case of sensing failure, especially for vehicle drive

application. For these reasons, design method of a sensorless controlled IPMSM is important.

In an IPMSM, permanent magnets (PM) have an effect on both induced back-electromotive force (BEMF) and spatial saliency distribution. Therefore, with high frequency signal injection method, the rotor position can be estimated [1]. As shown in Fig. 1, if voltage injection angle is  $0^\circ$  when the voltage is injected on the  $d$ -axis, the  $d$ -axis self-inductance should be the minimum value and  $dq$ -axis mutual-inductance must be zero. However, it is not easy to estimate the rotor

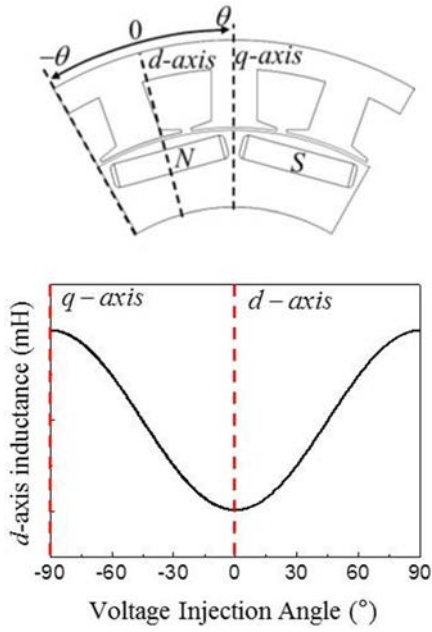


Figure1:  $d$ -axis inductance waveform under no-load condition

position under load conditions, since magnetic saturation and cross-coupling effect [2]-[5]. In this paper, the error of the rotor position estimation predicted by evaluating the shifting level of zero-crossing points of  $dq$ -axis inductances with a rotor position [4]. For this process, the fixed permeability method and  $d, q$ -axis transformation of inductance are conducted. Based on the procedure, some design factors are examined by finite element analysis (FEA). As a result, it is founded that the error of the rotor position estimation can be significantly decreased by means of the appropriate geometry design.

## 2 Calculating of The Inductances for Evaluating Saliency-based Sensorless Drive Feasibility

### 2.1 Fixed Permeability Method

The fixed permeability method is used for obtaining 3-phase self- and mutual-inductances [6]-[7]. Fig. 2 shows this procedure to find the inductances. Firstly, nonlinear FEA has to be done, considering permanent magnets and saturation of the core. The second step is fixing the permeability of the each element. After this, linear FEA is conducted with eliminating the PM. At this time, by injecting 1-phase coil with unit current, self- and mutual-inductance can be obtained. This procedure should be iterated,

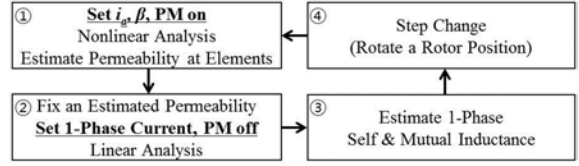


Figure2: Flow chart of the fixed permeability method

changing the rotor position because the waveform and zero-crossing point of the  $dq$ -axis inductance is varied with the rotor position and this variation cause the error of the rotor position estimation.

### 2.2 Matrix Transformation of the Inductances

With equation (1)~(3), a 3-phase inductance matrix determined by fixed permeability method can be transformed to the  $d, q$ -axis inductances depending on a voltage injection angle.

$$L_{AB} = \begin{bmatrix} L_A + L_B \cos 2\theta_r & -\frac{1}{2}L_A + L_B \cos 2\left(\theta_r - \frac{\pi}{3}\right) & -\frac{1}{2}L_A + L_B \cos 2\left(\theta_r + \frac{\pi}{3}\right) \\ -\frac{1}{2}L_A + L_B \cos 2\left(\theta_r - \frac{\pi}{3}\right) & L_A + L_B \cos 2\left(\theta_r + \frac{\pi}{3}\right) & -\frac{1}{2}L_A + L_B \cos 2\theta_r \\ -\frac{1}{2}L_A + L_B \cos 2\left(\theta_r + \frac{\pi}{3}\right) & -\frac{1}{2}L_A + L_B \cos 2\theta_r & L_A + L_B \cos 2\left(\theta_r - \frac{\pi}{3}\right) \end{bmatrix} + L_{ABh} \quad (1)$$

$$L'_{dq} = \frac{3}{2}T_{\theta_r} T_{dq} L_{AB} (T_{\theta_r} T_{dq})^T = \begin{bmatrix} L_{dd} & L_{dq} \\ L_{qd} & L_{qq} \end{bmatrix} \quad (2)$$

$$T_{\theta_r} = \begin{bmatrix} \cos \theta & \sin \theta \\ -\sin \theta & \cos \theta \end{bmatrix}, T_{dq} = \frac{2}{3} \begin{bmatrix} 1 & -\frac{1}{2} & -\frac{1}{2} \\ 0 & \frac{\sqrt{3}}{2} & -\frac{\sqrt{3}}{2} \end{bmatrix} \quad (3)$$

where  $L_{AB}$  is 3-phase inductances including harmonics  $L_{ABh}$  at stationary coordinate obtained by fixed permeability method,  $\theta_r$  means the position of the rotor, and  $T_{dq}$  and  $T_{\theta_r}$  are the  $d, q$ -axis transform and rotational transform coefficient.  $L_{dd}$  and  $L_{qq}$  are the  $d$  and  $q$ -axis self-inductance and

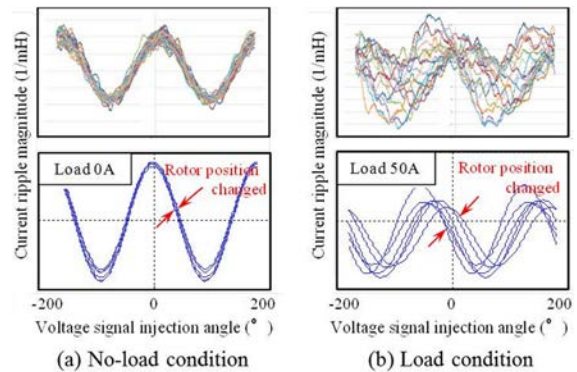


Figure3: Estimated current ripple (lower) and experimental results (upper)

$L_{dq}$  and  $L_{qd}$  are the  $dq$ -axis mutual-inductances. Fig. 3 illustrates the variation of the  $d$ -axis current ripple (inverse values of  $L_{dd}$ ) with the rotor position under no-load and load conditions.

### 3 Analysis of Design Factors for a Sensorless-oriented IPMSM

#### 3.1 Magnetic Load and Electric Load

An IPMSM for ideal sensorless drive should have the same  $dq$ -axis inductance waveforms as the rotor position changed under the load conditions. It requires sinusoidal flux distribution and the minimum flux distortion by armature reaction at the air gap. This means that sensorless-oriented machines have to be designed higher magnetic load than electric load as much as possible. Variation of  $dq$ -axis mutual-inductance waveforms with the rotor position as changing magnetic load are shown in Fig. 4. In the figure, different residual magnetic flux

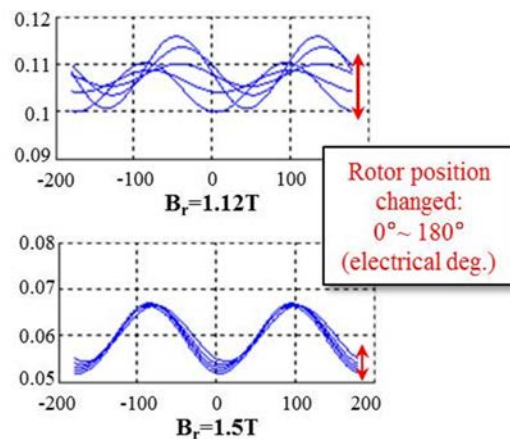


Figure4: Inductance waveforms as changing residual flux density ( $x$ -axis: voltage injection angle)

density is used representing for magnetic load. Equation (4) and (5) describes magnetic load and electric load.  $B$ ,  $L_{stk}$ ,  $N_{ph}$  and  $D_r$  mean flux density, stack length, number of turn phase and rotor diameter respectively. Pole-pair number and number of phase are  $p$  and  $m$ .

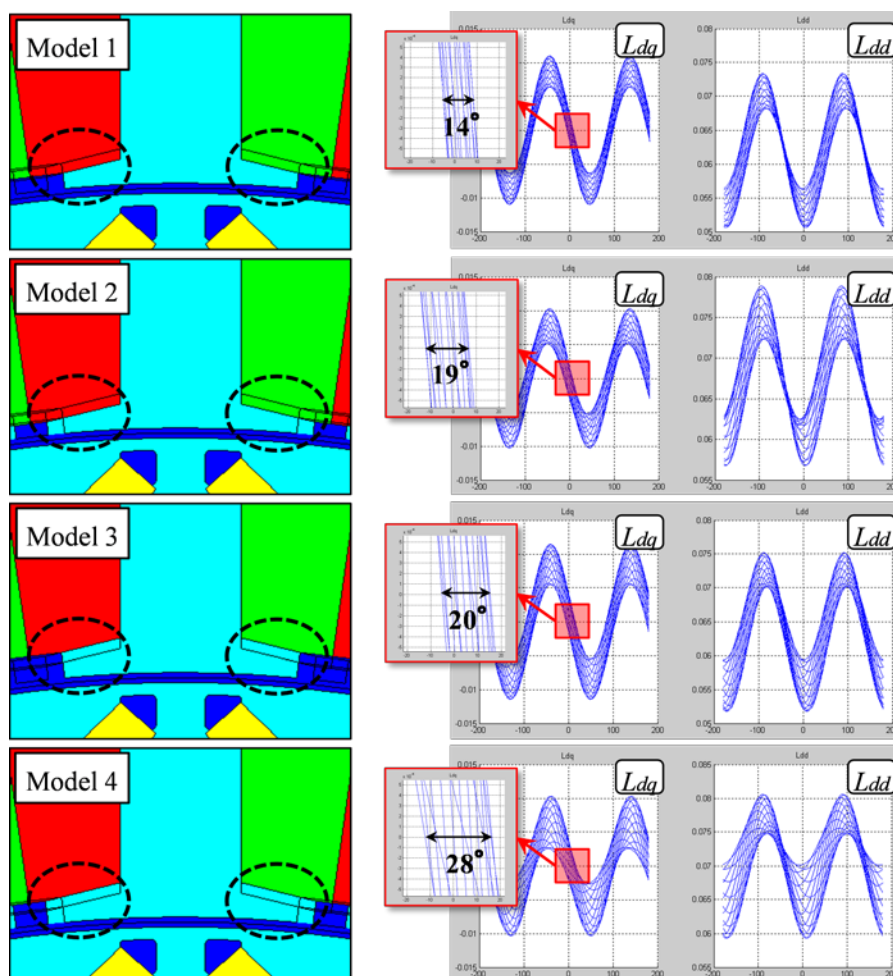


Figure5: Inductance waveforms of four different models and rotor position errors obtained by the inductances varied with the rotor position ( $x$ -axis: voltage injection angle)

$$\phi = B \times \frac{\pi D_r L_{stk}}{2p} \quad [Wb] \quad (4)$$

$$A = \frac{2mN_{ph}I}{\pi D_r} \quad [A/m] \quad (5)$$

### 3.2 Design Factors in a Stator

Slot open and thickness of the stator tooth-tip are examined as geometry design parameters to figure out their effects on the sensorless control. Fig. 5 shows the four different models and  $d$ -axis self- and  $dq$ -axis mutual-inductance waveforms varied with the rotor position under the maximum load conditions. All the models have the same rotor geometry, designed higher magnetic load than electric load as much as possible. Given the results, the rotor positions are detected much more precisely when the tooth-tip is shorter and thinner as model 1. It infers that saturation of the tooth-tip can be one of the key factors to design concentrated winding IPMSM for sensorless control.

## 4 Prototype

In this paper, the prototype (16pole-24slot, 115Nm-14kW), an IPMSM, applying chamfers to the stator tooth-tip of the model1, is proposed. The reason that chamfer was adopted is to saturate the tooth-tip more effectively as the results of the parameter analysis. Fig. 6 shows the proposed model and the  $dq$ -axis mutual-inductances varied with the rotor position. Estimated rotor position errors of the four different models in Fig. 5 and the prototype are compared in Table1. As you can see, the prototype has the minimum estimated position error due to the optimal shape of the tooth-tip.

## 5 Conclusion

This paper explained calculating process of  $d$ ,  $q$ -axis inductances accounting for cross-coupling effect to predict sensorless control feasibility. Based on the procedure, some geometry design factors were examined to clarify the design method of sensorless-oriented IPMSM with concentrated winding. As a result, it is found that the shape of the tooth-tip can be one of the key factors. Thus, based on the geometry parameter analysis results, the prototype is proposed, which has the most stable sensorless drive characteristics of the other models in the paper. Consequently, it validates that accuracy of the

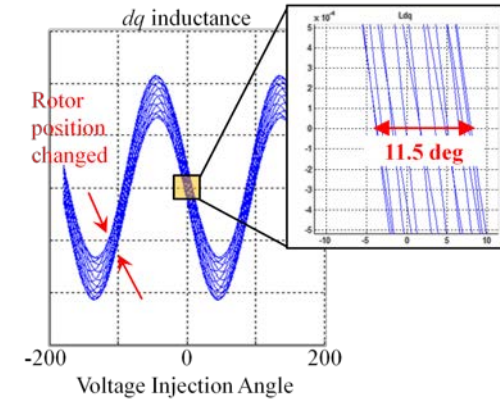
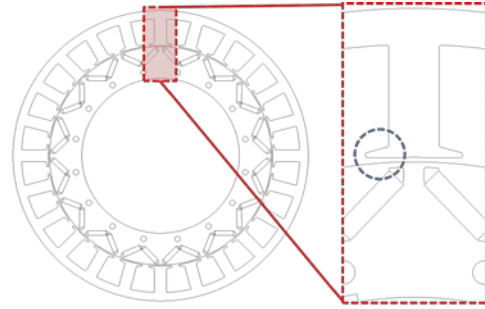


Figure6: Shape of the prototype and the  $dq$ -axis inductances under the maximum load conditions

Table1: Comparison of proposed models in the paper

|           | Shape of the tooth-tip (length/thickness) | Estimated position error (deg.) |
|-----------|---|---------------------------------|
| Model 1   | short/thin                                | 14                              |
| Model 2   | long/thin                                 | 19                              |
| Model 3   | short/thick                               | 20                              |
| Model 4   | long/thick                                | 28                              |
| Prototype | short/thin and chamfer                    | 11.5                            |

rotor position estimation can be improved by means of the proper geometry design of the machines.

## Acknowledgments

This research was supported by the MKE(The Ministry of Knowledge Economy), Korea, under the CITRC(Convergence Information Technology Research Center) support program (NIPA-2013-H0401-13-1008) supervised by the NIPA(National IT Industry Promotion Agency)

## References

- [1] S. M. Kim, J. I. Ha and S. K. Sul, *PWM switching frequency signal injection sensorless method in IPMSM*, Industrial

Applications, ISSN 0093-9994, 2012, 1576-1587

- [2] Y. Kano, T. Kosaka, N. Matsui and M. Fusitsuna, *Sensorless-oriented design of concentrated winding IPM motors for HEV drive application*, International Conference on Electrical machine (ICEM), ISBN 978-1-4673-0141-1, 2012, 2709-2715
- [3] Y. Li, Z. Q. Zhu, D. Howe and C. M. Bingham, *Modeling of cross-coupling magnetic saturation in signal-injection-based sensorless control of permanent-magnet brushless AC motors*, Magnetics, ISSN 0018-9464, 2007, 2552-2554
- [4] Z. Q. Zhu, Y. Li, D. Howe and C. M. Bingham, *Compensation for rotor position estimation error due to cross-coupling magnetic saturation in signal injection based sensorless control of PM brushless AC motor*, International Electric Machines and Drive Conference (IEMDC), ISBN 1-4244-0743-5, 2007, 208-213
- [5] N. Bianchi and S. Bolognani, *Influence of rotor geometry of an IPM motor on sensorless control feasibility*, Industrial Applications, ISSN 0093-9994, 2007, 87-96
- [6] J. K. Tangudu, T. M. Jahns, A. M. El-Refaie, and Z. Q. Zhu, *Segregation of torque components in fractional-slot concentrated-winding interior PM machines using frozen permeability*, Energy Conversion Congress and Exposition (ECCE), ISBN 978-1-4244-2893-9, 2009, 3814-3821
- [7] S. H. Chai, B. H. Lee, J. P. Hong, S. K. Sul and S. M. Kim, *Design of IPMSM having high power density for position sensorless operation with high-frequency signal injection and the method of calculating inductance profile*, International Conference on Electrical Machines and System (ICEMS), ISBN 978-1-4577-1044-5, 2011, 1-5



Seung-Hee Chai received Bachelor's degree in mechanical engineering from Hanyang University, Korea in 2009. Currently he is pursuing Ph.D. degree in automotive engineering from Hanyang University, Korea. His research interests are design of electric machines and optimization.



Jung-Pyo Hong received Ph.D. degree in electrical engineering from the Hanyang University, Korea, in 1995. From 1996 to 2006, he was professor of Changwon National Univ., Changwon, Korea. Since 2006 he has been working as a professor in the Hanyang University, Korea. His research interests are the design of electric machines, optimization and numerical analysis of electromechanics.

## Authors



Myung-Seop Lim received Bachelor's degree in mechanical engineering from Hanyang University, Korea in 2012. Currently he is pursuing Master's degree in automotive engineering from Hanyang University, Korea. His research interests are design of electric motors for vehicle applications and sensorless drive.